

# Cross-Line Characterization for Capacitive Cross Coupling in Differential Millimeter-Wave CMOS Amplifiers

Korkut Kaan Tokgoz, Kimsrun Lim, Yuuki Seo, Seitarou Kawai, Kenichi Okada,  
and Akira Matsuzawa

Tokyo Institute of Technology, Department of Physical Electronics, 2-12-1-S3-27  
Oookayama, Meguro-ku, Tokyo, 152-8552, Japan, E-mail: korkut@ssc.pe.titech.ac.jp

**Abstract**—An electrically symmetric cross-line and its characterization are proposed for capacitive cross coupling in differential amplifiers. The characterization of the device is done using two structures. L-2L method is applied to achieve virtual-thru connection of Ground-Signal-Signal-Ground (GSSG) pads and fixtures used in cross-line characterization structures. Pad parasitics are modeled with T-model which provides more accurate results than  $\Pi$ -model. Characterization of cross-line is done using one structure and verified with the other. Comparisons show well agreement in terms of four-port S-parameter responses up to 67 GHz.

**Index Terms**—Capacitive cross coupling, characterization, CMOS, cross-line, differential, mm-wave.

## I. INTRODUCTION

The unlicensed 9 GHz bandwidth around 60 GHz frequency region has enabled high-data-rate wireless transceivers. Furthermore, CMOS process has several advantages compared to compound semiconductor processes [1]. Use of single-ended, or differential circuits are possible for a transceiver system. For instance, in [1] power amplifier and low-noise amplifier are designed as single-ended to decrease area, increase flexibility on layout. On the other hand, differential amplifiers are also used for RF amplifiers, local oscillator buffers, especially considering transceivers with complex modulation schemes. Moreover, fully differential transceiver architecture can also be implemented [2]. Differential amplifiers in these applications have vital roles, and neutralization techniques can be used for higher gain, low power consumption, and decreased area [1], [2]. Capacitive cross coupled amplifier is a topology for neutralization technique, for which an illustration is given in Fig. 1. Symmetry for differential amplifiers is important for decreased phase and amplitude imbalance between the two differential signals, and decreased mode conversions between common and differential modes. Although the schematic shown in Fig. 1 is symmetrical, in the layout the crossing part could be asymmetrical. Due to these reasons, a cross-line is designed for capacitive cross coupled differential amplifier to decrease phase and amplitude imbalance as in Fig. 2. In Section II, this structure is explained with the structures used for characterization of this device. Section III describes virtual-thru de-embedding method for GSSG pad

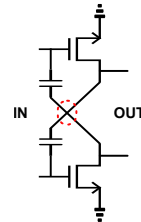


Fig. 1. An illustration for capacitive cross coupled differential amplifier (asymmetrical crossing in red dashed circle).

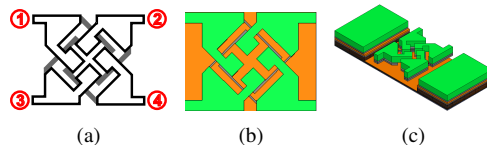


Fig. 2. Cross-line structure (a) port numbering, (b) top view (green areas are top and gray areas are lower metal, orange areas are first two metal layers for ground), and (c) bird-eye-view.

characterization. Section IV presents experimental results.

## II. CROSS-LINE AND CHARACTERIZATION STRUCTURES

Fig. 2(a) illustrates the cross-line. White areas present top metal layer and lower metal layer connected with vias. Moreover, gray areas present the lower metal layer connecting port 1 to 4 and port 2 to 3. Note that the structure is not fully symmetric considering physical layout, however, it is almost electrically symmetrical. Due to symmetry and reciprocity properties of the structure, the simplified S-parameters can be given as;

$$S_{CCC} = \begin{bmatrix} S_{11} & S_{12} & S_{13} & S_{14} \\ S_{12} & S_{11} & S_{14} & S_{13} \\ S_{13} & S_{14} & S_{11} & S_{12} \\ S_{14} & S_{13} & S_{12} & S_{11} \end{bmatrix} \quad (1)$$

One can observe that cross-line can be described using four S-parameters. Hence, two characterization structures are implemented. A general representation for the two characterization structures is provided in Fig. 3(a). Leftmost

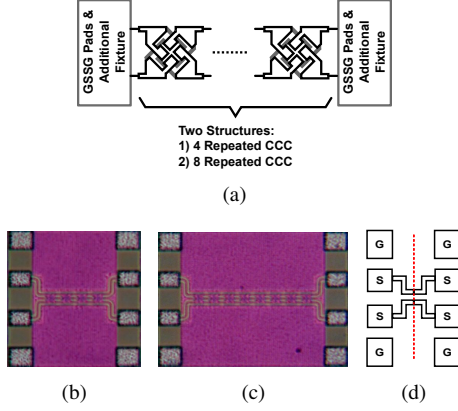


Fig. 3. Characterization structures (a) a general representation, (b) four cross-line repeated chip photo, (c) eight repeated chip photo, (d) virtual connection of fixtures.

and rightmost cross-line for both structure are connected to GSSG pads with fixtures based on CPWs. In one characterization structure, four cross-line are connected to each other, and eight in the other, to decrease errors from de-embedding of pads and fixtures. The values of four and eight are selected to easily calculate only the fixture effects using virtual-Thru (L-2L) of left and right fixtures with pads are shown in Fig. 3(d). To avoid four-port T-parameter based calculations and lessen the burden, mixed-mode S-parameters are used. Mixed-mode S-parameters can be calculated in general as;

$$[S_{MM}] = [M][S][M]^{-1} = \begin{bmatrix} S_{dd} & S_{dc} \\ S_{cd} & S_{cc} \end{bmatrix} \quad (2)$$

where  $[S_{MM}]$  is the mixed-mode S-parameter representation of a four-port network having  $[S]$ ,  $S_{dd}$  and  $S_{cc}$  are pure differential and common modes,  $S_{dc}$  and  $S_{cd}$  are the two conversion modes. Moreover,  $[M]$  is given in the following equation ( $I$  is two by two identity matrix).

$$[M] = \frac{1}{\sqrt{2}} \begin{bmatrix} I & -I \\ I & I \end{bmatrix} \quad (3)$$

Since the four-port networks used in here have symmetry and reciprocity properties, theoretically there is no conversion modes. Thus, one can divide mixed-mode of the network into two separate two-port networks. T-parameters of four and eight repeated crossing structure for differential mode can be written as;

$$[T]_{4U,dd} = [T]_{LP,dd} [T]_{F,dd} [T]_{C,dd}^4 [T]_{F,dd} [T]_{RP,dd} \quad (4)$$

$$[T]_{8U,dd} = [T]_{LP,dd} [T]_{F,dd} [T]_{C,dd}^8 [T]_{F,dd} [T]_{RP,dd} \quad (5)$$

The subscripts LP, RP, F, and C are for left-, right-pad, fixture CPWs, and cross-line. By using the following equation differential response of virtual-thru connection of fixtures can be calculated as;

$$[T]_{PF,dd} = [T]_{4U,dd} [T]_{8U,dd}^{-1} [T]_{4U,dd} \quad (6)$$

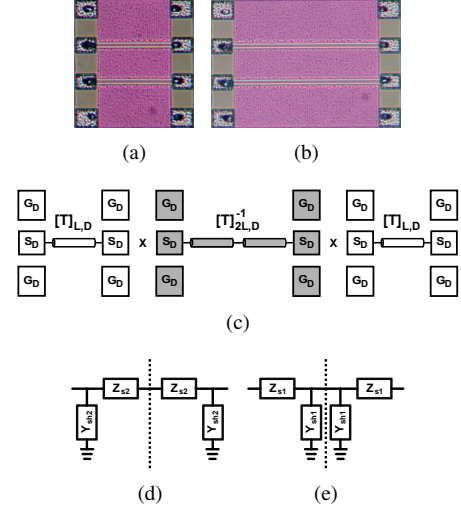


Fig. 4. Virtual-thru GSSG de-embedding (a) network with 200  $\mu\text{m}$  CPWs, (b) network with 400  $\mu\text{m}$  CPWs, (c) virtual-thru differential mode extraction (same is done for common mode), (d)  $\Pi$ -model for pads, and (e) T-model for pads.

$$[T]_{PF,dd} = [T]_{LP,dd} [T]_{F,dd} [T]_{F,dd} [T]_{RP,dd} \quad (7)$$

where subscript PF is related with left-pad, fixtures and right-pad combinations. One can calculate the common mode of the fixtures with pads responses using the same set of equations (replace “dd” with “cc”). To calculate cross-line one needs to de-embed the pad parasitics and fixture effects. The fixture effects can be solved assuming symmetry property for fixtures after de-embedding pad responses in both pure modes.

### III. VIRTUAL-THRU GSSG DE-EMBEDDING METHOD

In [3], simple thru de-embedding method is presented for four-port networks. However, this method is affected by undesired coupling between probes. For this reason, similar to [4], virtual-thru (L-2L) method for GSSG de-embedding is established. Two four-port networks with CPWs having 200 and 400  $\mu\text{m}$  lengths are established. Chip photos for these two networks are provided in Fig. 4. Four-port single-ended S-parameters are converted to mixed-mode S-parameters. Again, there is no mode conversion. These four-port networks can be divided into common and differential two-port networks. Using the method shown in Fig. 4(c), one can calculate virtual connection of left and right pad in terms of differential response. Similarly common mode response can be obtained. Using virtual responses of both modes, pad parasitics for two different modes can be assumed  $\Pi$ - (Fig. 4(d)), or T-model (Fig. 4(e)). After measurements are done using four-port VNA, method is followed and virtual-thru response is calculated. Pad parasitics for both modes are calculated using Y-parameters for  $\Pi$  pad model, and Z-parameters for T-model. It can be observed from Fig. 5(a) that T-model for

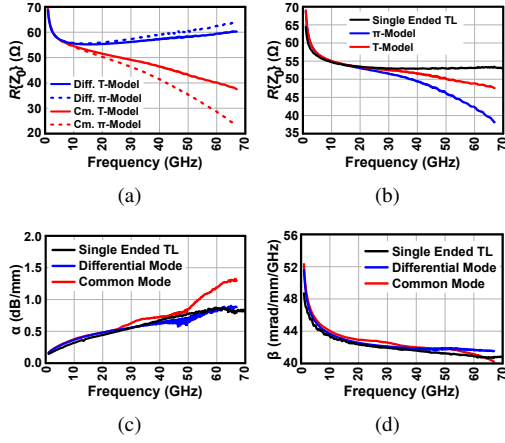


Fig. 5. CPW parameters for pure modes in comparison with two-port CPW characteristics (a) characteristic impedance of common (red lines) and differential (blue lines) for  $\Pi$ - (dashed lines), and T-model (solid lines), (b) mean values of pure modes characteristic impedance, (c)  $\alpha$ , and (d)  $\beta$ .

both modes provides more accurate results than  $\Pi$ -model, based on the characteristic impedance response of both modes. Since there is large ground plane between CPWs, pure mode responses after de-embedding should be close to two-port CPW characteristics, this can be observed in  $\alpha$  (Fig. 5(c)) and  $\beta$  (Fig. 5(d)) results after de-embedding. Both modes responses are close to each other, and also to two-port CPW characteristics obtained before this work. T-model is assumed for both modes in order to be used in de-embedding needed for cross-line characterization.

#### IV. EXPERIMENTAL RESULTS

From Eq. (7) pad parasitics responses can be de-embedded in terms of differential and common mode, and remaining response is two cascaded fixture response. One can solve for one fixture responses for two modes easily. To calculate cross-line results, from Eq. (4) pad parasitics and fixtures are de-embedded from left and right side. Left response is  $[T]_{C,dd}^4$  for differential mode and  $[T]_{C,cc}^4$  for common mode. One cross-line can be calculated easily for both modes. Four-port response of cross-line can be calculated by applying mixed-mode to single-ended S-parameter transformation. In order to verify obtained results, eight repeated structure (Fig. 3(c)) response is reconstructed in a simulation environment with calculated responses. The reconstructed model results are compared with measurements and provided in Fig. 6. Single-ended S-parameters of this four-port network has symmetry and reciprocity properties there are four different S-parameter results. It can be observed that model and measurement results well-match with each other up to 67 GHz, which validates characterized cross-line results.

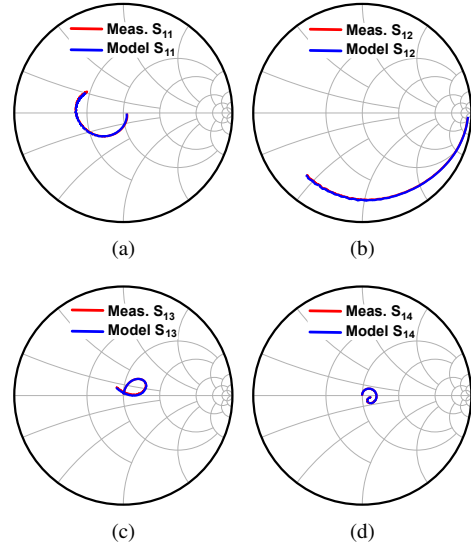


Fig. 6. S-parameter comparison between model (blue lines) and measurement (red lines) results of eight repeated cross-line up to 67 GHz (a)  $S_{11}$ , (a)  $S_{12}$ , (a)  $S_{13}$ , and (a)  $S_{14}$ .

#### V. CONCLUSION

An electrically symmetrical cross-line is introduced. Characterization of this structure is done using properties of mixed-mode S-parameters. A virtual-thru de-embedding method is used for GSSG pad parasitics calculation by applying L-2L method. This method is also applied to calculate the fixtures used in cross-line characterization structures. De-embedding of pad parasitics and fixtures are done on four repeated cross-line structure to calculate for one. Using characterized cross-line, fixtures and pad parasitics, eight repeated structure is reconstructed in a simulation environment and the results are compared with measurements. Comparisons show that there is a good match between model and measurements up to 67 GHz.

#### ACKNOWLEDGMENT

This work is partially supported by MIC, SCOPE, MEXT, STARC, STAR and VDEC in collaboration with Cadence Design Systems, Inc., Mentor Graphics, Inc., and Agilent Technologies Japan, Ltd.

#### REFERENCES

- [1] K. Okada, *et al.*, "Full Four-Channel 6.3-Gb/s 60-GHz CMOS Transceiver With Low-Power Analog and Digital Baseband Circuitry," *IEEE JSSC*, vol.48, no.1, pp.46-65, Jan. 2013.
- [2] Z. Wang, *et al.*, "A CMOS 210-GHz Fundamental Transceiver With OOK Modulation," *IEEE JSSC*, vol.49, no.3, pp.564-580, Mar. 2014.
- [3] S. Amakawa, *et al.*, "A Simple De-Embedding Method for Characterization of On-Chip Four-Port Networks," *Proc. AMC 2008*, pp.99-103, 2009.
- [4] N. Li, *et al.*, "Evaluation of a Multi-Line De-embedding Technique up to 110 GHz for Millimeter-Wave CMOS Circuit Design," *IEICE Trans. Fundam. Electron.*, Vol. E93-A, No. 2, pp.431-439, Feb. 2010.